

# Neutron tomography of geological samples – preliminary results.

L. Longridge<sup>1</sup>, F. C. de Beer<sup>2</sup>, L. Coney<sup>3</sup>, P. Ogilvie<sup>4</sup>, S. Webb<sup>5</sup>

1. University of the Witwatersrand, South Africa, luke.longridge@wits.ac.za
2. Research and Development Division, Necsa, South Africa, Frikkie.DeBeer@necsa.co.za
3. SADPMR Laboratory, Mintek, South Africa, louise.coney@mintek.co.za
4. University of the Witwatersrand, South Africa, arcpaula2@gmail.com
5. University of the Witwatersrand, South Africa, susan.webb@wits.ac.za

## ABSTRACT

Neutron tomographic imaging has been conducted on a variety of geological samples, including migmatitic metapelite, suevitic breccia, as well as mafic granulite, in order to investigate the success of this technique in non-destructively distinguishing their component minerals in three-dimensions. Preliminary results indicate that coarse textures found in these samples are clearly resolved, but  $\mu\text{m}$ -scale resolution of mineral distribution is not yet possible. The variable composition of minerals in geological samples due to solid solution results in overlapping attenuation coefficients for some minerals, and these minerals may be indistinguishable using neutron tomography. Hydrous minerals and voids present in samples are well resolved, and volumes of component phases in samples can be easily calculated, provided these phases are resolvable.

**Key words:** Neutron tomography, textural investigation, migmatite, suevite, granulite.

## INTRODUCTION

Neutron tomography is a technique with the potential to image geological samples on a  $\mu\text{m}$ -scale in three-dimensions. This technique is an extension of neutron radiography, which exploits the interaction (and attenuation) of thermal neutrons with the nucleus of an atom. Different nuclides attenuate neutrons passing through a sample to differing degrees, and thus areas of varying composition can be imaged by mapping the degree of attenuation of these areas. The attenuation coefficient of a material is dependent on the composition and density of a material, and theoretical attenuation coefficients for a material can be calculated provided its composition and the density are known (Domanus, 1995). Thermal neutron attenuation coefficients for minerals common in the samples investigated are shown in Table 1. Since many minerals display solid-solution, they may have overlapping ranges of attenuation coefficients, resulting in very low contrasts between minerals within the neutron tomograms. For example, quartz, feldspar and cordierite have similar attenuation coefficients, as do orthopyroxene and clinopyroxene. It may therefore be difficult to distinguish between these minerals through neutron tomography. However, since hydrogen has a very high neutron attenuation coefficient, hydrous minerals (e.g. biotite) have correspondingly high

attenuation coefficients and are likely to be well imaged and resolved by neutron tomography.

Mineral	Attenuation Coefficient ( $\text{cm}^{-1}$ )
Quartz	0.277
Biotite	0.57-0.72
K-feldspar	0.263-0.273
Plagioclase feldspar	0.249-0.292
Garnet	0.287-0.538
Cordierite	0.261-0.278
Orthopyroxene	0.354-0.512
Clinopyroxene	0.320-0.398

**Table 1. Thermal neutron attenuation coefficients**

This paper presents the preliminary results obtained from neutron tomography investigation of a variety of geological samples. These results indicate that three-dimensional resolution of different phases in geological samples using this technique is successful, but that the composition and grain size of the sample will determine how well the phases are resolved.

## EXPERIMENTAL SETUP

Tomographic imaging of the samples was carried out at the SAFARI-1 nuclear research reactor at Necsa, Pretoria. The samples were mounted on a rotating stage,

taking care to place the sample centrally on the stage to avoid any eccentricity on the axis of rotation. During a 360° rotation of the sample, 375 neutron radiograph projections of each sample were taken, an example of which is shown in Figure 1 using the photon image generated by a neutron scintillation screen (6LiF/ZnS:Cu,Al,Au) and digitally imaged using a Peltier-cooled CCD camera. These radiographs were reconstructed into three-dimensional tomographic images using Octopus reconstruction software and visualised through VGStudio MAX-2.1 software with a theoretical resolution of ~100 µm. These greyscale images show areas of higher attenuation as lighter grey and those with lower attenuation as darker shades of grey (Figure 1). Details of the experimental setup are given by De Beer (2005).

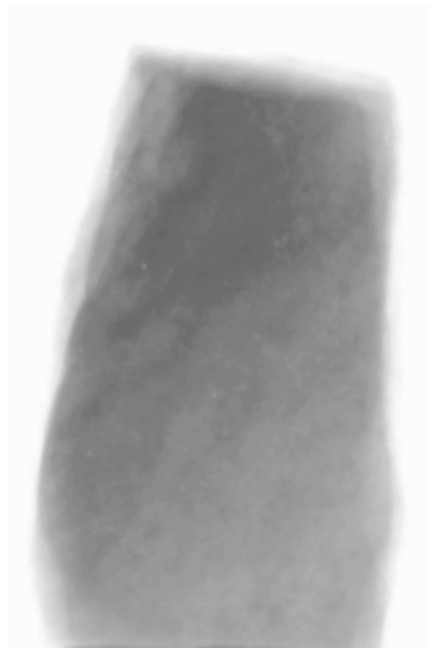


**Figure 1.** Neutron radiograph of sample SK9a.

## RESULTS

A number of different geological samples were selected for this study. Although this is not a comprehensive study of all possible rock types, the study provides preliminary results as to what rock types provide the best contrast and images. Rock types include pelitic migmatites, impact breccias, suevite, granulite, anorthosite, and kimberlite. A description of selected samples is provided below, as well as an evaluation of the success of the tomographic imaging performed in this study.

### LID004

Sample LID004 (Figure 2) is a pelitic migmatite from the Central Zone of the Neoproterozoic Damara Orogen in Namibia, which has experienced upper amphibolite- to granulite facies metamorphism (Masberg et al.,

1992). This sample is a slice through the axial region of a dm-scale fold (the trace of this fold is indicated by the white line in Figure 2). In the inner portion of this fold, anatectic migmatite is developed as narrow (0.5 mm - 1 mm) leucosome veins parallel to the axial plane of the fold (Figure 2). This core region contains the assemblage quartz-biotite-plagioclase-cordierite-sillimanite, with minor amounts of garnet, and is fairly coarse-grained (0.4 mm – 1 mm). The outer portion of the fold does not show leucosome development, and consists predominantly of fine-grained quartz and biotite (~0.2 mm), with large garnet porphyroblasts (1 mm – 5 mm), which are often surrounded by haloes of biotite (Figure 2).

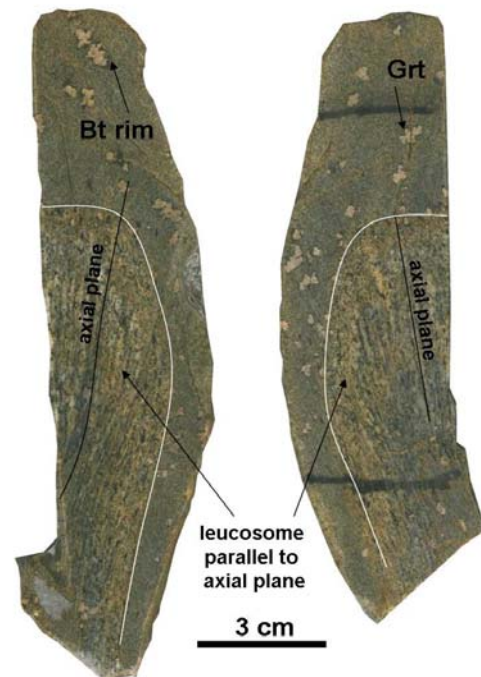


**Figure 2.** Photograph of the two cut surfaces of LID004 (sample has been cut perpendicular to the fold hinge line).

Tomographic imaging of this sample (originally in greyscale) shows that the sample can be subdivided into three areas, corresponding to low, intermediate, and high attenuation values (Figure 3). Low attenuation values (yellow in Figure 3) correspond to areas with large amounts of quartz and feldspar, whilst high attenuation (red in Figure 3) values indicate the presence of hydrous biotite. Intermediate attenuation values (blue in Figure 3) are an uncertain assemblage of garnet and cordierite, and possibly fine-grained quartz and biotite. In the core of the sample, the axial-planar fabric of the fold is clearly distinguished, and alternating bands of biotite-rich and quartz and feldspar-rich material can be distinguished, suggesting axial planar development of leucosome in this sample. The fairly coarse nature of the sample in this core area enables good textural resolution. However, in the fine-grained outer portion of the fold, the sample appears to

be largely composed of intermediate attenuation material, despite the fact that petrographic inspection shows that this is fine-grained biotite (high attenuation) and quartz (low attenuation). Garnet is not resolved, but the biotite haloes surrounding the garnet porphyroblasts are clearly defined, as is the zone of coarse-grained biotite along the boundary between the core and outer portion of the fold (Figure 3).

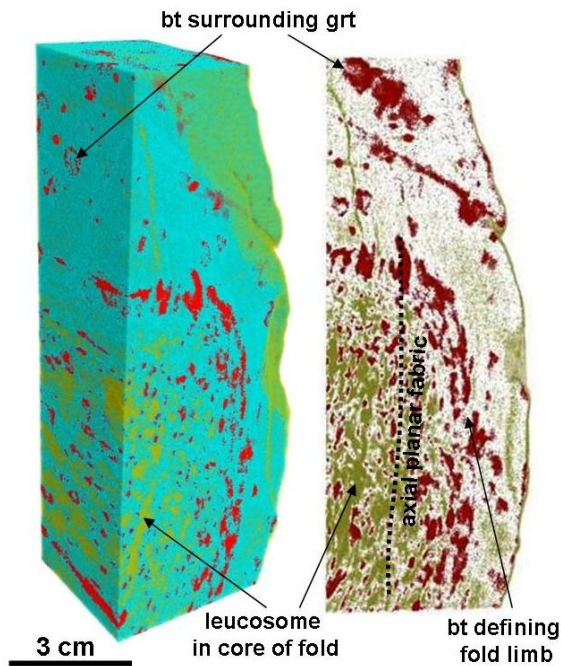


**Figure 3.** False-colour tomographic images of sample LID004, showing a three-dimensional view of the sample, as well as the ~0.5 mm slice through the sample, perpendicular to the fold hinge line.

### BS-16

Sample BS-16 (Figure 4) is from the 1.07 Ma Bosumtwi impact structure, Ghana (see Koeberl et al., 2007; Koeberl and Reimold, 2005). The crater is medium-sized and complex in its morphology, and BS-16 is a suevite from north of the crater, collected in 2007 (Coney, 2009). Suevite is defined as “polymict impact breccia that includes melt particles (glassy or crystallized) in a mostly clastic matrix containing lithic and mineral clasts in various stages of shock metamorphism” (see Stöffler and Grieve, 2007). The sample consists of a matrix-supported suevite. Matrix comprises approximately 47 vol% of the sample, and the bulk of the rest of the specimen consists chiefly of melt particles (35 vol%), with schist, granite, quartz and feldspar clasts (Figure 4). The melt particles are highly vesiculated and contain quartz particles. Following tomographic imaging of BS-16, the sample can again be divided into low, intermediate, and high attenuation areas (yellow, blue and red in Figure 5, respectively). The highly vesiculated melt particles are clearly defined

as low attenuation areas, and can be distinguished from the matrix and clasts in the sample (Figure 5).

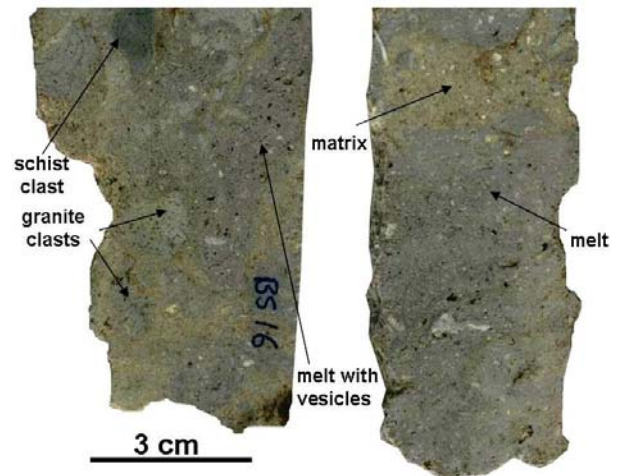


**Figure 4.** Photograph of the two cut surfaces of BS16, showing grey, vesiculated melt particles (containing quartz clasts), yellow matrix, and clasts of schist and granite.

The melt is calculated to make up 69.6 vol% of the sample, substantially more than estimates from petrographic, two-dimensional analysis. Clasts of schist (rich in biotite) are also clearly distinguishable as high attenuation material, and make up 2.3 vol% of the sample. The remainder of the sample (28.1 vol%) is material which produces intermediate attenuation values, and may be either matrix or granite. Additionally, the total volume of voids in the sample can be calculated using VGStudio MAX-2.1. The majority of these voids are seen to occur within the low attenuation melt particles (Figure 5), and are vesicles in the melt. These vesicles make up 1.24 vol% of the melt particles.

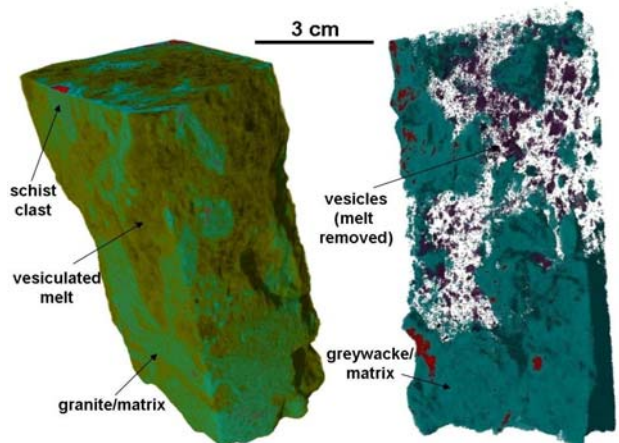


**Figure 5.** False-colour tomographic images of sample BS16, showing a three-dimensional projection of the surface of the sample, and a ~10 mm slice through the sample, with low attenuation melt removed.

**SK9a**

Sample SK9a (Figure 6) is a granulite from the Archaean Basement Complex exposed in the core of the Vredefort Dome, South Africa which includes numerous NW-SE trending, metapelitic, metagreywacke, metamafic and lesser metaironstone xenoliths (interpreted as greenstone remnants; Stepto, 1999) enclosed within 3120-3100 Ma tonalitic and trondhjemitic gneisses. The metasedimentary granulites comprise stromatic and locally massive garnet-biotite-cordierite/orthopyroxene restites occurring as isolated, discontinuous outcrops between 5 and 12 km from the centre of the dome. SK9a is a stromatic orthopyroxene-bearing metagreywacke comprising a fine- to medium-grained assemblage of garnet (20-30 vol%), orthopyroxene (10-20 vol%), biotite (5-10 vol%), quartz, plagioclase, K-feldspar and ilmenite. (Figure 6). Peak metamorphic conditions are: 870-885 °C and 7.1-7.7 kbar during D3 at 3.08 Ga (Ogilvie, pers. comm.). Overprinting the coarse-grained peak assemblage are deformation features related to the Vredefort impact event. These include the presence of pseudotachylitic breccias, recrystallised planar deformation features (PDFs) in quartz, planar fractures (PFs) in garnet, and kink-banding of biotite. Plagioclase and K-feldspar exhibit recrystallisation to microcrystalline aggregates after diaplectic glass. Corona textures are also sectorally developed around garnet. They comprise complex multi-layered product symplectites and bands. Orthopyroxene vermicule grain size varies from 5-100 µm. Average vermicule size is around 10-20 µm. Layer thickness varies from 50 to 350 µm. Generally, thicker corona layers and coarser vermicules occur in coronas after garnet and biotite.

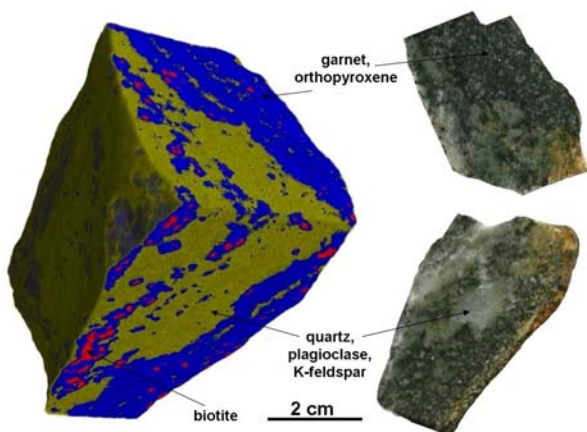


**Figure 6. False-colour three-dimensional tomographic image of SK9a, with photographs of two of the samples cut surfaces for comparison.**

Tomographic imaging of SK9a shows that high attenuation biotite in the sample is clearly resolved, and the stromatic fabric of the granulite can clearly be distinguished as alternating quartz-feldspar or garnet-orthopyroxene layers (Figure 6). However, µm-scale

details such as the symplectite corona textures around garnet, or kink-banding in biotite, are not resolved.

**CONCLUSIONS**

This preliminary investigation shows the success of neutron tomography on a variety of geological samples. The overlapping attenuation coefficients of minerals means that although coarse textural relationships between clearly resolvable minerals can be investigated in three-dimensions, the technique is currently unable to resolve µm-scale details. Hydrous minerals (such as biotite) are well resolved using neutron tomography, and textures which are defined by hydrous minerals are the best candidates for investigation using this technique. Additionally, voids in samples (such as vesicles in glass) can be clearly imaged and quantified using neutron tomography.

**REFERENCES**

- De Beer, F.C., 2005, Characteristics of the neutron/X-ray tomography system at the SANRAD facility in South Africa: Nuclear Instruments and Methods in Physics Research A, 542, 1-8.
- Domanus, J.C., 1992 Practical Neutron Radiography, Springer Publishers, ISBN 0792318609, 9780792318606
- Coney, L., 2009, Mineralogy and geochemistry of the impact breccias of the Bosumtwi impact structure, Ghana: Genesis and secondary processes: Ph.D Thesis, University of the Witwatersrand, Johannesburg.
- Koerberl C. and Reimold W.U., 2005, Bosumtwi impact crater, Ghana (West Africa): An updated and revised geological map, with explanations: Jahrbuch der Geologischen Bundesanstalt, Wien (Yearbook of the Geological Survey of Austria) Vienna, 145, 31-70 and 1 map, 1:50,000.
- Koerberl C., Milkereit B., Overpeck J. T., Scholtz C. A., Amoako P. Y. O., Boamah D., Danuor S., Karp T., Kueck J., Hecky R. E., King J. W. and Peck J., 2007, An international and multidisciplinary drilling project into a young complex impact structure: The 2004 ICDP Bosumtwi Crater Drilling Project - An overview: Meteoritics and Planetary Science, 42, 483-511.
- Masberg, H.P, Hoffer, E. and Hoernes, S, 1992, Microfabrics indicating granulite-facies metamorphism in the low-pressure central Damara Orogen, Namibia: Precambrian Research, 55, 243-257.
- Stöffler, D., and Grieve, R.A.F., 2007, Impactites, Chapter 2.11, in Metamorphic Rocks: A Classification and Glossary of Terms, Recommendations of the International Union of Geological Sciences, Fettes, D. and J. Desmons, J., eds, Cambridge University Press, Cambridge, 82-92, 111-125, and 126-242.
- Stepto, D., 1979. A geological and geophysical study of the central portion of the Vredefort Dome structure. Ph.D Thesis, University of the Witwatersrand, Johannesburg.